Volume 374, issue 2 1 February 2007 ISSN 0378-4371

PHYSICA A
Recognized by the European Physical Society
STATISTICAL MECHANICS AND ITS APPLICATIONS

Available online at
ScienceDirect
www.sciencedirect.com
http://www.elsevier.com/locate/physa

Available online at www.sciencedirect.com
ScienceDirect
Physica A 374 (2007) 715–729
PHYSICA A
www.elsevier.com/locate/physa

A multi-interacting-agent model for financial markets

Sílvio M. Duarte Queirós, E.M.F. Curado, F.D. Nobre*

Centro Brasileiro de Pesquisas Físicas, Rua Xavier Sigaud 150, 22290-180 Rio de Janeiro - RJ, Brazil

Received 18 May 2006
Available online 18 August 2006

Abstract

Microscopic models, which resemble random magnetic systems, have been used recently in the literature for the description of financial markets. In the present work, a model with many interacting agents, similar to an Ising random magnet with infinite-range interactions, is investigated. The introduction of a local-field term, depending on the absolute value of a magnetization-like parameter—which measures the volatility of a financial market—leads to a significant improvement with respect to previously studied models in the literature. By investigating the return time series, we show that several features, characteristic of real financial markets, are better reproduced by the present model. In particular, within this approach one is able to provide a proper behavior for the following properties: (i) the power-law tails and the nonzero skewness of the probability distribution of returns; (ii) the exponential decay of the two-time autocorrelation function of returns, typical of high-frequency financial data; (iii) the so-called ''leverage effect'', which corresponds to a negative correlation between past returns and future volatility.

Keywords: Econophysics; Financial markets; Time-series analysis

1. Introduction

The techniques developed in the area of statistical mechanics, which used to be regularly employed for studying physical systems, have been applied recently in the investigation of a wide variety of complex systems, composed by many interacting elements. As a result of this, new interdisciplinary areas of investigation have emerged, and among these, one may single out the rapidly-growing subject of econophysics [1–4].

Financial markets have been chosen by many physicists as a paradigmatic complex system, characterized by the intricate character often exhibited, where every part of the system seems to depend on every other [5]. Some basic quantities in these systems are the price returns, which are associated to given relative price changes, as well as the volatilities, which correspond to the absolute values (or amplitudes) of returns. From

*Corresponding author.
E-mail addresses: sdqueiro@cbpf.br (S.M.D. Queirós), evaldo@cbpf.br (E.M.F. Curado), fdnobre@cbpf.br (F.D. Nobre).

0378-4371/$ - see front matter © 2006 Elsevier B.V. All rights reserved.
doi:10.1016/j.physa.2006.07.042

empirical studies, several aspects are nowadays considered as inherent of real competitive financial markets, and some of them are listed below.

(i) The time series of price returns exhibits bursts (which resemble chaotic bursts that appear in intermittent non-linear dynamical systems), characteristic of extreme events [5,6].
(ii) The distribution of returns is non-Gaussian [7–9], and presents a slight asymmetry around the origin, usually associated to risk aversion [2], characterized either by different power-law (or different amplitude) behaviors on each side, i.e., positive and negative tails [6].
(iii) The two-time autocorrelation function of price returns decays exponentially, for a time scale of the order of a few minutes, and after that, one observes a noise level, i.e., no correlations [6].
(iv) The two-time autocorrelation function of volatilities displays asymptotically a power-law behavior, signaling long-memory effects in this quantity. Such a ''persistence'' is sometimes referred in the literature as ''volatility clustering'' [5].
(v) Past returns and future volatilities present negative correlations, the so-called ''leverage effect'', which means that volatilities tend to increase when the corresponding prices drop, and vice versa [10].

One of the main challenges of the physical approach to economic systems consists in the proposal of theoretical models, which could describe properly the behavior of real financial markets. Based on the empirical facts, many attempts have been presented in the literature, which were able to reproduce some of the above-mentioned characteristics, but not all of them. Some of the recently proposed models approach the financial markets from a macroscopic point of view, and are built from differential equations, like those models based on Langevin-like equations [11–13] and non-linear Fokker–Planck equations [14,15]. However, a recent and very promising class of theoretical models try to approach the financial markets from a microscopic point of view, being defined as a complex system, characterized by many interacting subunits [16–22]. Based on the facts that every subunit should feel the presence of all remaining ones, and that each pair of subunits should interact in a different manner, the microscopic models proposed resemble those models used in statistical physics for the description of random magnets, for which there is a vast literature available [23–25].

In the present work we define a microscopic model, based on random interactions among the agents, considering a term that measures the volatility of the financial market. We show that this model presents substantial improvements with respect to previous microscopic models in the literature. In particular, such a model is able to cope, satisfactorily, with most of the empirical aspects mentioned above. In the next section we define the model and the numerical procedure to be used. In Section 3 we discuss the results obtained from our model, comparing them with some empirical data. Finally, in Section 4 we present our main conclusions.

2. The model and numerical procedure

Let us consider a system composed by N agents that take decisions under the influence of the external environment, as well as of the remaining agents. Inspired by some recently used microscopic models in econophysics, and also on well-known models of statistical mechanics, let us assign to each agent a two-state variable $\sigma_i = \pm 1$ $(i = 1, 2, \ldots, N)$, corresponding to the decision for buying $(+1)$ or selling (-1) a share of a traded stock, or commodity, at discrete time steps t. The state of agent i at time $t + 1$ depends on the actions of other agents, as well as of random events and volatilities, which will be incorporated in a local field at time t,

$$I_i(t) = \frac{1}{N-1}\sum_{j\neq i} A_{ij}(t)\sigma_j(t) + h_i(t) - B_i|x(t)|. \tag{1}$$

In the equation above, $\{A_{ij}(t)\}$ represent the time dependent interactions among agents, whereas $\{h_i(t)\}$ are external fields, which take into account the random effects of the environment. The summation $\sum_{j\neq i}$ applies to all remaining agents, which would correspond, within the statistical-mechanics language, to infinite-range interactions.

The average quantity,

$$x(t) = \frac{1}{N}\sum_{i=1}^{N}\sigma_i(t), \tag{2}$$

represents the difference between the number of buying and selling decisions (i.e., between demand and supply). The last term in Eq. (1) considers the amplitude of variations, at time t, of the variable $x(t)$. For $B>0$ (which will be the case analyzed herein) this term contributes to adjust the agents in such a way to avoid large variations on $x(t)$. Therefore, it carries an important ingredient of financial markets: the so-called aversion to risk.

Let us now consider $S(t)$ as representing a given time series of prices or market index values; it is widely used in the literature [12,26] that the time rate of price changes is proportional to both $x(t)$ and $S(t)$,

$$\frac{\mathrm{d}S(t)}{\mathrm{d}t} \propto x(t)S(t). \tag{3}$$

From the equation above, one gets, after time discretization,

$$\ln S(t') - \ln S(t) \propto \sum_{n=0}^{m-1} x(t+n\,\Delta t)\Delta t,$$

where $t' = t + m\,\Delta t$. Considering $m = 1$, one obtains

$$x(t) \propto \ln S(t+\Delta t) - \ln S(t), \tag{4}$$

which shows that the variable $x(t)$ is directly related to the return over a time scale Δt (that will be considered herein as $\Delta t = 1$). The absolute value $|x(t)| \propto |\ln S(t+\Delta t) - \ln S(t)|$ is usually called volatility, and represents the magnitude of price changes [1]. Therefore, the last term in Eq. (1) introduces a dependence of the local field on the volatility, taking into account the aversion to risk. For positive (negative) values of B_i, the agent i is induced to sell (buy) when the volatility increases. It is important to mention that for $B_i = 0$, the model defined above recovers the one introduced in Ref. [20].

This system may evolve in time following a certain dynamics. Let us consider herein the heat-bath dynamics, for which the variables $\{\sigma_i(t)\}$ are updated according to the probabilistic rule,

$$\sigma_i(t+1) = \begin{cases} 1 & \text{with probability } p_i(t), \\ -1 & \text{with probability } 1-p_i(t), \end{cases} \tag{5a}$$

where

$$p_i(t) = \{1 + \exp[-2I_i(t)]\}^{-1}. \tag{5b}$$

It should be emphasized that the variables $\{\sigma_i(t)\}$ may be updated in a sequential (asynchronous) form, i.e., a single variable $\sigma_i(t)$ is updated at once, or in a parallel (synchronous) form, i.e., all variables $\{\sigma_i(t)\}$ are updated at a given time. Within both procedures, a time step (usually called a Monte Carlo step) corresponds to the updating of the whole set of variables $\{\sigma_i(t)\}$ $(i = 1, 2, \ldots, N)$.

Employing the random-magnet-problem language, the model defined in Eq. (1) represents an infinite-range-interaction model, for which the mean-field treatment yields the correct result for a sequential updating of a given ergodic dynamics of the model, in the long-time and thermodynamic limits. Let us consider, for the moment, a mean-field approach for the above model, within the sequential updating; if one considers,

$$A_{ij}(t) = A\xi(t)\ (\forall i \neq j); \quad h_i(t) = h\zeta(t)\ (\forall i); \quad B_i(t) = B\ (\forall i), \tag{6}$$

where $\xi(t)$ and $\zeta(t)$ are random variables in time, uniformly distributed in the interval $[-1, 1]$, one gets a local field that does not depend on the site index i,

$$I(t) = A\xi(t)x(t) + h\zeta(t) - B|x(t)|. \tag{7}$$

Therefore, the average value of a variable σ at time $t+1$, may be easily calculated for the set of rules defined in Eqs. (5),

$$[\sigma(t+1)]_{\mathrm{av}} = (+1)p(t) + (-1)[1-p(t)] = 2p(t) - 1 = \tanh[I(t)].$$

Within the mean-field approximation, one can identify the above average value with the return variable $x(t+1)$,

$$[\sigma(t+1)]_{\mathrm{av}} = \frac{1}{N}\sum_{i=1}^{N}\sigma_i(t+1) \equiv x(t+1),$$

in such a way that

$$x(t+1) = \tanh[I(t)] = \tanh[A\xi(t)x(t) + h\zeta(t) - B|x(t)|]. \tag{8}$$

It is important to mention that although the mean-field treatment of the above model, within a parallel updating, leads, in general, to a different thermodynamics when compared to the one of the well-known infinite-range interaction model, the recursion relation of Eq. (8) may also be used within the parallel updating [27,28]. In fact, one expects that a parallel updating of a microscopic system of interacting agents should mimic better a real financial system than the corresponding sequential updating. Usually, in present-day financial markets, all agents are interconnected through computer networks in such a way that, in a small time interval, many agents take decisions almost simultaneously.

From Eq. (8), by considering a given initial condition, $x(0)$, one generates the time series of returns $x(t)$, in the thermodynamic limit, from which one may define a probability distribution of returns $P(x)$. We have checked that, for the parameters (A, h, B) within the range of interest of real financial markets, the magnitudes for the returns gets restricted to small values (typically, $|x|<0.2$). In this case, considering $|A\xi(t)x(t) - B|x(t)| + h\zeta(t)| \ll 1$, Eq. (8) may be linearized,

$$x(t+1) \approx A\xi(t)x(t) + h\zeta(t) - B|x(t)|. \tag{9}$$

In general, the maps of Eqs. (8) and (9) may lead to different regimes, like chaotic ones, or those characterized by well-defined fixed points, depending on the choices for the parameters (A, h, B) (see the appendix, for a detailed analysis of these maps). The onset of chaos, signalled by the maximum Lyapunov exponent becoming positive, occurs therefore at a general threshold surface, which may be defined as $A^*(h, B)$. For $B = 0$, both maps fall in a broad class of maps which have been investigated extensively [29–31]. In the case $h = 0$, for a uniformly distributed noise $\xi(t)$ in the interval $(-1, 1)$, there is a fixed point at $x = 0$ for $A < A^*(0, 0)$ $[A^*(0, 0) = e = 2.718\ldots]$, whereas for $A \geqslant A^*(0, 0)$ this fixed point loses stability and one enters into the chaotic region. The introduction of a small $h > 0$ is sufficient to reduce this threshold value to $A^*(h, 0) = 1$ [29–31]. As discussed in the appendix, for the case $B > 0$ one gets a qualitatively similar picture, in such a way that for the typical value $B = 0.22$, considered in the next section, the onset of chaos takes place at approximately the same threshold values as in the case $B = 0$.

One may easily obtain the parameter B from Eq. (9); in fact, multiplying Eq. (9) by $x(t)$, one gets,

$$x(t+1)x(t) \approx A\xi(t)x^2(t) + h\zeta(t)x(t) - B|x(t)|x(t).$$

Applying time averages to both sides of the above equation, taking into account the fact that $\xi(t)$ and $\zeta(t)$ are independent random variables in time, randomly distributed in the interval $[-1, 1]$ (whose averages in time are zero), one gets the simple relation,

$$B \approx -\frac{\langle x(t+1)x(t)\rangle}{\langle |x(t)|x(t)\rangle}, \tag{10}$$

where $\langle\,\rangle$ denote time averages. Therefore, the parameter B may be easily estimated for an empirical time series with elements $\{x(t)\}$ within the range of validity of the linear approximation of Eq. (9), and it is directly related to the correlation function $\langle x(t+1)x(t)\rangle$.

In the next section we verify numerically that, similarly to what happens in the case $B = 0$ [32,33], the tails of the probability distribution associated with the linearized map of Eq. (9) also follow the power-law scaling

$$P(x) \sim |x|^{-\alpha-1}, \tag{11}$$

for small positive values of B, with $B \gg h > 0$, and $|x| \gg h > 0$. These conditions restrict the ranges to be used for the parameters B and h, for an appropriated description of a real market. In principle, one may have two different exponents (α and β) for the two sides of $P(x)$, i.e., $x<0$ and $x>0$, respectively. However, as shown in the appendix, $\alpha = \beta$, and a simple equation may be obtained (considering $h = 0$), relating A, B and α [cf., Eq. (A.13)],

$$\frac{(A-B)^{1+\alpha} + (A+B)^{1+\alpha}}{2A(1+\alpha)} = 1. \tag{12}$$

Obviously, Eq. (12) corresponds to a leading contribution in an expansion for small values of h, in such a way that higher-order terms may become negligible if one chooses conveniently small enough values of h.

Therefore, if one holds an empirical time series with an associated probability distribution following the power-law of Eq. (11), and whose elements $\{x(t)\}$ fall within the range of validity of the linear approximation of Eq. (9), one may, at first, measure the exponent α by a proper fit of the empirical data to the scaling behavior of Eq. (11). Hence, the parameter B may be estimated from Eq. (10) and finally, parameter A may be obtained from Eq. (12). In this way, by fixing h to a small arbitrary value, one finds, as an approximation, the best pair of parameters (A, B) in order to mimic the real system under consideration.

From Eq. (8), apart from the time series of returns $x(t)$, one may also define a time series of volatilities, $v(t) = |x(t)|$. The two-time autocorrelation functions of such quantities are of particular interest in econophysics,

$$C_x(\tau) = \frac{\langle x(t)x(t+\tau)\rangle - \langle x(t)\rangle^2}{\langle x^2(t)\rangle - \langle x(t)\rangle^2}, \tag{13}$$

$$C_v(\tau) = \frac{\langle v(t)v(t+\tau)\rangle - \langle v(t)\rangle^2}{\langle v^2(t)\rangle - \langle v(t)\rangle^2}. \tag{14}$$

Another important quantity, relevant for the investigation of the leverage effect, is the leverage correlation function [10], which corresponds to the correlation between past returns and future volatilities,

$$\mathscr{L}(\tau) = \frac{\langle x(t)v(t+\tau)\rangle - \langle x(t)\rangle\langle v(t)\rangle}{\langle v(t)\rangle^2}. \tag{15}$$

In the next section we present and discuss our results.

3. Results and discussion

In this section we show the substantial improvements, of the present model, with respect to previous microscopic models in the literature. For that, we have compared the results produced from data of our model with those obtained from the 1-min return time series of the 30 most important individual stocks of Dow Jones index (the so-called DJ30). Our data refer to the period from July 1, 2004, up to December 31, 2004, corresponding to nearly 50 000 points for each time series. By employing the method explained in the previous section, we were able to obtain the values of B for each of the individual time series of DJ30; we verified a diversity of values of B within a range varying approximately from $B = 0.10$ up to 0.35, leading to an average value $B = 0.22 \pm 0.05$. For each time series, one may construct a histogram of returns; by considering a superposition of such histograms, one may define an "average probability distribution", associated with the returns of DJ30 in this period of time. Such a probability distribution is slightly asymmetrical and is represented in Fig. 1(a); the abscissae are rescaled by their respective variance. In Fig. 1(b) we exhibit a log–log plot of this probability distribution, showing a good agreement with the asymptotic scaling form of Eq. (11), with approximately the same exponent for both positive and negative values of x. In this case, we found a good fitting with the following distribution,

$$P(x) = P(0)(1 + \gamma_{\pm}x^2)^{-\mu_{\pm}}, \tag{16}$$

where, the $+$ $(-)$ sign applies to positive (negative) returns and in the asymptotic regime, $\mu_{\pm} = (\alpha_{\pm} + 1)/2$. The fitting for negative values of returns (squares), represented in Fig. 1(b) by a dashed line, is undiscernible from

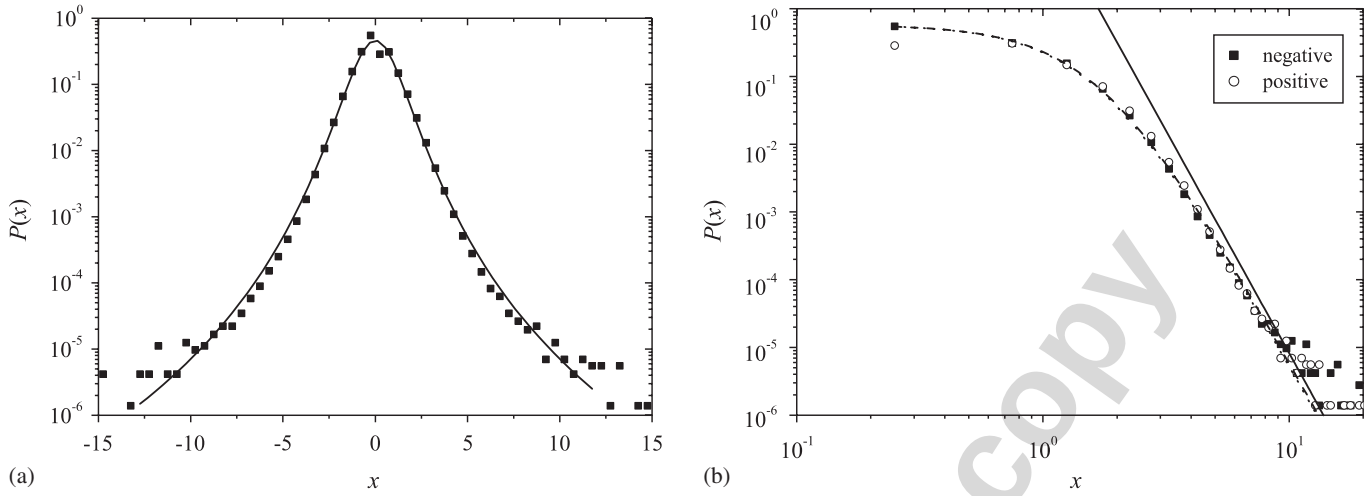

Fig. 1. (a) Probability distribution of returns $x(t)$ (rescaled by their respective variance), from data of DJ30 (see text); the full line corresponds to the distribution of Eq. (16), as described in the text. (b) Log–log plot of the probability distribution in (a), showing the asymptotic behavior of Eq. (11); the straight line presents a slope -6.56, which would correspond to an exponent $\alpha = 5.56$. The squares (circles) correspond to negative (positive) return values and are fitted by the same distribution as in (a), represented herein by a dashed (dotted) line. These two fittings (dashed and dotted lines) are undiscernible to a naked eye.

the one of positive returns (circles), represented in Fig. 1(b) by a dotted line. For positive returns, we have used the Hill estimator [34] in order to find the tail exponent, $\alpha_+ = 5.57 \pm 0.08$; from a standard non-linear fitting procedure, we obtained $P(0) = 0.582 \pm 0.001$, $\gamma_+ = 0.864 \pm 0.004$, with the goodness parameters, chi squared, $\chi^2 = 1.24 \times 10^{-6}$, and reduced chi squared, $R^2 = 0.99855$. For negative returns, the same procedure leads to $\alpha_- = 5.54 \pm 0.06$, $P(0) = 0.582 \pm 0.001$, $\gamma_- = 0.837 \pm 0.003$, $\chi^2 = 1.1 \times 10^{-6}$, and $R^2 = 0.99871$. One observes the same exponent α, within the error bars, for both sides of the distribution, which may be well approximated by $\alpha = 5.56 \pm 0.08$ [cf. straight line in Fig. 1(b)]. The asymmetry of the distribution is essentially assigned to the parameters $\gamma_\pm$ which are slightly different from one another. By substituting the values $\alpha = 5.56 \pm 0.08$ and $B = 0.22 \pm 0.05$ in Eq. (12), one finds $A = 1.3 \pm 0.06$; these represent the best set of values, of the parameters in the present theoretical model, for an appropriate description of the above-mentioned empirical data. This shows that the volatility-like term in the local field of Eq. (1), with $B > 0$, is indeed very important for a proper description of real data.

Let us now consider data generated from our theoretical model. It is important to mention that, for the parameters (A, h, B) used herein, the magnitudes for the returns gets restricted to small values, in such a way that the two maps [Eqs. (8) and (9)] lead essentially to the same quantitative results; an example of such a good quantitative agreement is illustrated in the Appendix, through the computation of the Lyapunov exponents. In the analysis that follows, we consider time series generated by using the values $A = 1.5$ and $h = 0.01$ (which represent typical values used in Ref. [20]), as well as $B = 0.25$ (which is very close to the average value of DJ30, mentioned above), for the parameters of Eq. (6). Whenever comparing our theoretical data with the above-mentioned DJ30 data, we shall use the set of parameters $A = 1.3$, $B = 0.22$, and $h = 0.01$. In addition to that, some analyses will also be carried for several values of the parameter B. For the one-dimensional map of Eq. (8), we have always employed the initial condition $x(0) = 0$, although we have verified that the particular choice of $x(0)$ is irrelevant for the general behavior of the time series.

First, we have generated a time series of returns $x(t)$ from a numerical simulation, for finite values of N, by means of both sequential and parallel updatings of the spin variables within the heat-bath algorithm, as defined above. In the case of a parallel updating, for a very small number of agents, one gets time series characterized by large fluctuations, as shown in Fig. 2(a) for $N = 50$. Nevertheless, for increasing values of N, the amplitude of the fluctuations decreases, and one observes well-defined bursts, even for small sizes, like $N = 500$, as shown in Fig. 2(b). Therefore, in the thermodynamic limit ($N \to \infty$), one expects a time series of returns consisting of small fluctuations around zero ($|x| \ll 1$), with the appearance of bursts randomly in time. In the case of the sequential updating, we have noticed a slow convergence to the thermodynamic limit, in such a way that, up to the values of N investigated (typically $N \cong 5000$), we have not identified clearly the presence

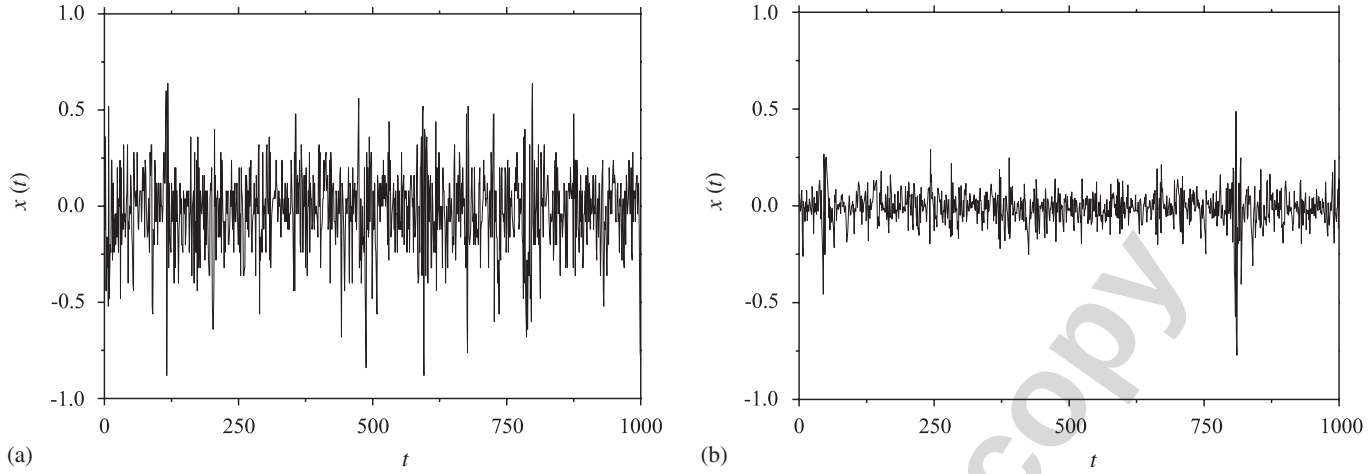

Fig. 2. The time series of returns $x(t)$ generated from a parallel updating of N agents, for the cases (a) $N = 50$; (b) $N = 500$. The parameters of Eq. (6) were considered as $A = 1.5$, $h = 0.01$, and $B = 0.25$.

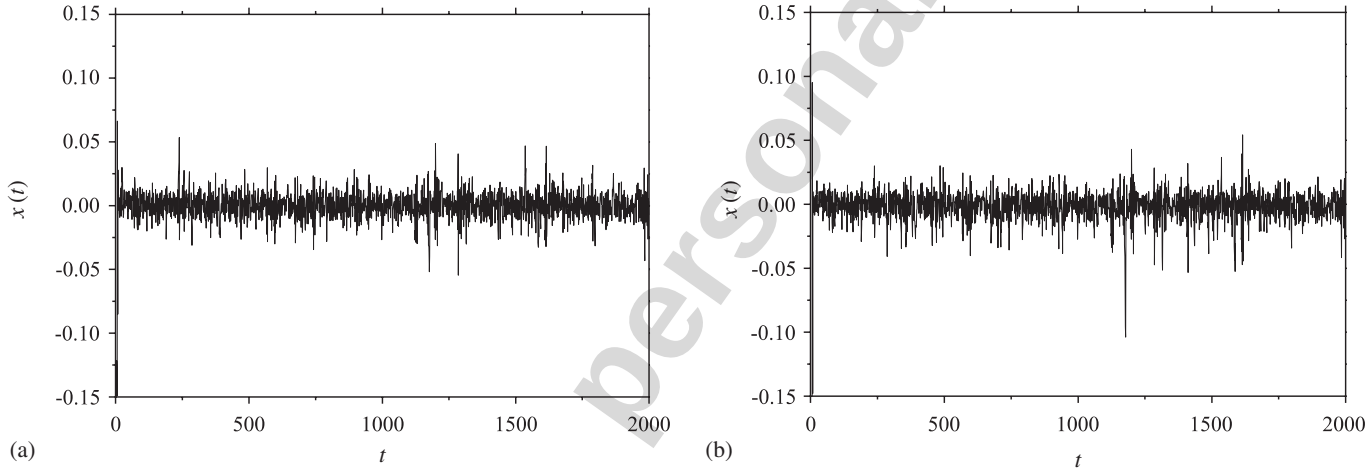

Fig. 3. The time series of returns $x(t)$ generated from the map of Eq. (8), for the cases (a) $B = 0$; (b) $B = 0.25$. In both cases, the values $A = 1.5$ and $h = 0.01$ were used.

of bursts. However, in the long-time limit, the sequential updating of spins leads, in the thermodynamic limit, to the one-dimensional map of Eq. (8).

In Fig. 3 we exhibit the time series, obtained from iteration of the map of Eq. (8), for $B = 0$ [Fig. 3(a)] and $B = 0.25$ [Fig. 3(b)]. In both cases, one observes the presence of chaotic bursts, characteristic of extreme events, in agreement with the empirical results [5,6], as well as with the results of the simulations shown in Fig. 2. Also, one notices that the magnitude of the chaotic bursts increases for $B > 0$. It is important to notice that, in either case of Fig. 3, the amplitude of returns remains small, i.e., $|x| \ll 1$, as expected from the simulations of Fig. 2, in the thermodynamic limit; in addition to that, this result supports the use of the linear approximation [Eq. (9)] for the map of Eq. (8). From now on, our results will refer to time series obtained from the iteration of the map of Eq. (8).

In Fig. 4 we exhibit the probability distribution of returns for $B = 0$ [Fig. 4(a)] and $B = 0.25$ [Fig. 4(b)]; the abscissae are rescaled by their respective variance. It is a well-known fact that the probability distribution of returns of a real financial market does not follow a Gaussian distribution [5,6]. As an example of this, we have the probability distribution of the above-mentioned DJ30 data, fitted by the function of Eq. (16). In the case of Fig. 4(a), we have verified that the return distribution was well fitted by a symmetric power-law [cf. Eq. (16)] with a tail exponent obtained through a Hill estimator, $\alpha = 3.84 \pm 0.04$, and a standard non-linear fitting

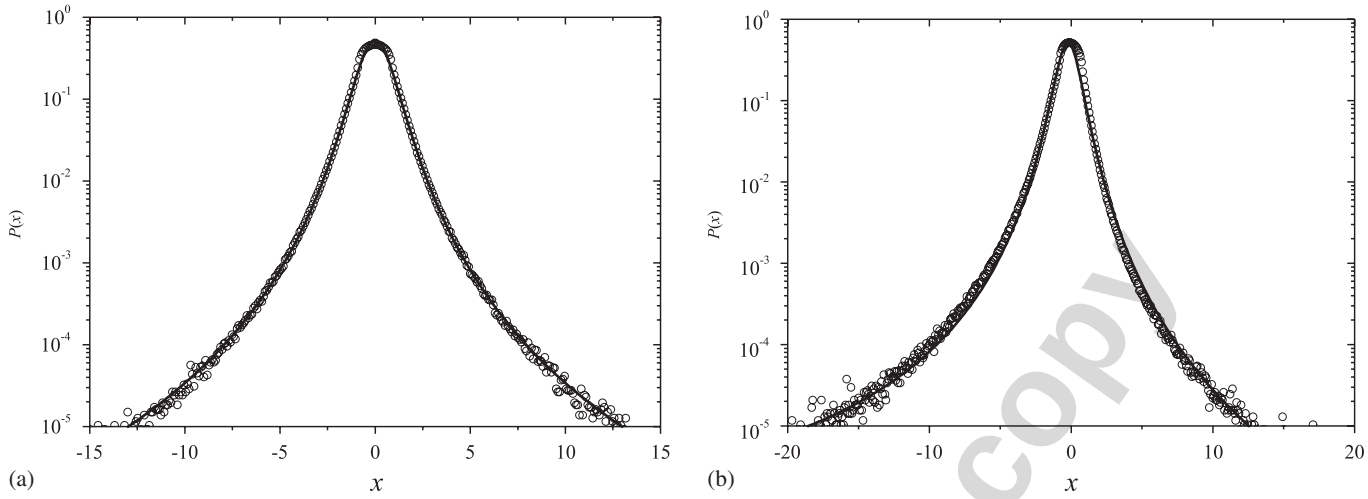

Fig. 4. Probability distributions of returns $x(t)$ (rescaled by their respective variance), for the cases (a) $B = 0$; (b) $B = 0.25$. In both cases, the values $A = 1.5$ and $h = 0.01$ were used. Nice fittings are represented in each case, by (almost undiscernible) full lines. In (a) the full line represents a symmetric Tsallis distribution [cf. Eq. (17)], whereas in (b) the full line stands for a Tsallis distribution with a nonzero skewness [cf. Eq. (18)].

leading to $P(0) = 0.532 \pm 0.003$, $\gamma_+ = \gamma_- = 0.57 \pm 0.03$, with the goodness parameters $\chi^2 = 1.4 \times 10^{-4}$ and $R^2 = 0.9847$. Since Tsallis distributions [35,36] are closely related to dynamical systems containing additive and multiplicative noises [37], like the one treated herein, we shall present as an equivalent fitting, a symmetric Tsallis distribution,

$$p_q(x) = \left[\frac{(q-1)\beta}{\pi(3-q)}\right]^{1/2} \frac{\Gamma(q/(q-1))}{\Gamma((q+1)/2(q-1))} \frac{1}{[1+\beta((q-1)/(3-q))x^2]^{1/(q-1)}}, \tag{17}$$

represented in Fig. 4(a) by a full line. Within this fitting, one gets the entropic index $q = 1.42 \pm 0.01$ and $\beta = 0.85 \pm 0.03$, with the same goodness parameters specified above. The probability distribution of Fig. 4(b) displays an asymmetry, similarly to what happens in real financial systems; in this case, the best fitting, which applies to the whole range of returns (positive and negative values), was found through a Tsallis distribution, with a nonzero skewness,

$$p_q(x) = p_q(0) \frac{1}{[1+\beta((q-1)/(3-q))(x^2+cx^3)]^{1/(q-1)}}, \tag{18}$$

represented in Fig. 4(b) by a full line. For this fitting, we found $\beta = 1.68 \pm 0.05$, $c = 1.62 \pm 0.04$, $q = 1.47 \pm 0.03$, and $p_q(0) = 0.515 \pm 0.003$ ($\chi^2 = 1.2 \times 10^{-3}$ and $R^2 = 0.9454$).

As mentioned before, the return probability distributions of real markets are asymmetric, presenting different behaviors for the positive and negative tails [6]. Therefore, the model defined in Eq. (1), with $B > 0$, leads to a probability distribution of returns that approaches real systems better than the corresponding model without the volatility-like term ($B = 0$). In order to show evidence of this, we have applied our theoretical model by considering the parameters $A = 1.3$, $B = 0.22$ (which are the values we obtained from DJ30 data), and $h = 0.01$. The resulting probability distribution displays an asymmetry, similarly to what happens in real financial systems, and may be fitted by the function of Eq. (16), with $P(0) = 0.457 \pm 0.007$, and $\gamma_+ = 0.44 \pm 0.08$, $\alpha_+ = 5.47 \pm 0.04$ ($\chi^2 = 4.5 \times 10^{-4}$ and $R^2 = 0.95199$), for positive returns, whereas $\gamma_- = 0.20 \pm 0.06$, $\alpha_- = 5.40 \pm 0.03$ ($\chi^2 = 1.7 \times 10^{-4}$ and $R^2 = 0.9880$), for negative returns. The tail exponents of each side coincide (considering the error bars), in such a way that one may define a single exponent, $\alpha = 5.44 \pm 0.06$, which agrees, within the error bars, with the estimate for the DJ30 data, $\alpha = 5.56 \pm 0.08$. Such large values for the exponent α are compatible with finite variances in the probability distribution of returns. One expects that by considering larger-horizon series of returns, this distribution should approach a Gaussian, in agreement with recent works [6,38], instead of a Lévy distribution, as previously conjectured [39]. However,

such an approach occurs more slowly than expected if one analyzes convolutions in the return variables; this effect is attributed to the dependence of returns on volatility, which presents long-lasting correlations [40,41].

Let us now consider the two-time autocorrelation functions, as defined in Eqs. (13) and (14). In Fig. 5 we exhibit the absolute values of $C_x(\tau)$, for $B = 0$ [Fig. 5(a)] and $B = 0.25$ [Fig. 5(b)], as well as those of $C_v(\tau)$, for the same values of B [Figs. 5(c) and (d)]. In the autocorrelation function of returns, the well-known exponential decay for small values of τ, peculiar of intra-day empirical data [5,6], can only be found if $B > 0$; in Fig. 5(b) one finds the characteristic decay time $\tau^* = 8$ [in arbitrary time units, as defined by Eq. (8)]. The case $B = 0$, for which one finds a noisy behavior in $C_x(\tau)$ for all values of τ, is only appropriate for the description of inter-day empirical data (i.e., large values of τ). An entire satisfactory agreement with the expected empirical behavior for the correlation function $C_x(\tau)$, i.e., exponential decay for small τ (intra-day data) and noisy behavior for larger values of τ (inter-day data) is only obtained if $B > 0$. However, in what concerns the autocorrelation function of volatilities, the volatility-like term in Eq. (1) does not change qualitatively its behavior. Figs. 4(c) and (d) are both in disagreement with the empirical results, that yield a power-law decay for $C_v(\tau)$ [5,6]. In addition to that, we have verified numerically that correlation functions of powers (i.e., moments) of absolute returns did not exhibit multiscaling properties, in contrast to what has been found from empirical data [42–44].

It is possible to define a correlation function $C_x(\tau)$, associated with the DJ30 data (see Fig. 6), as a sample average over its respective constituents. In this way, each square in Fig. 6 corresponds to an average of $C_x(\tau)$ over the 30 stocks of DJ30. From this data, one gets the characteristic decay time (see dashed straight line in

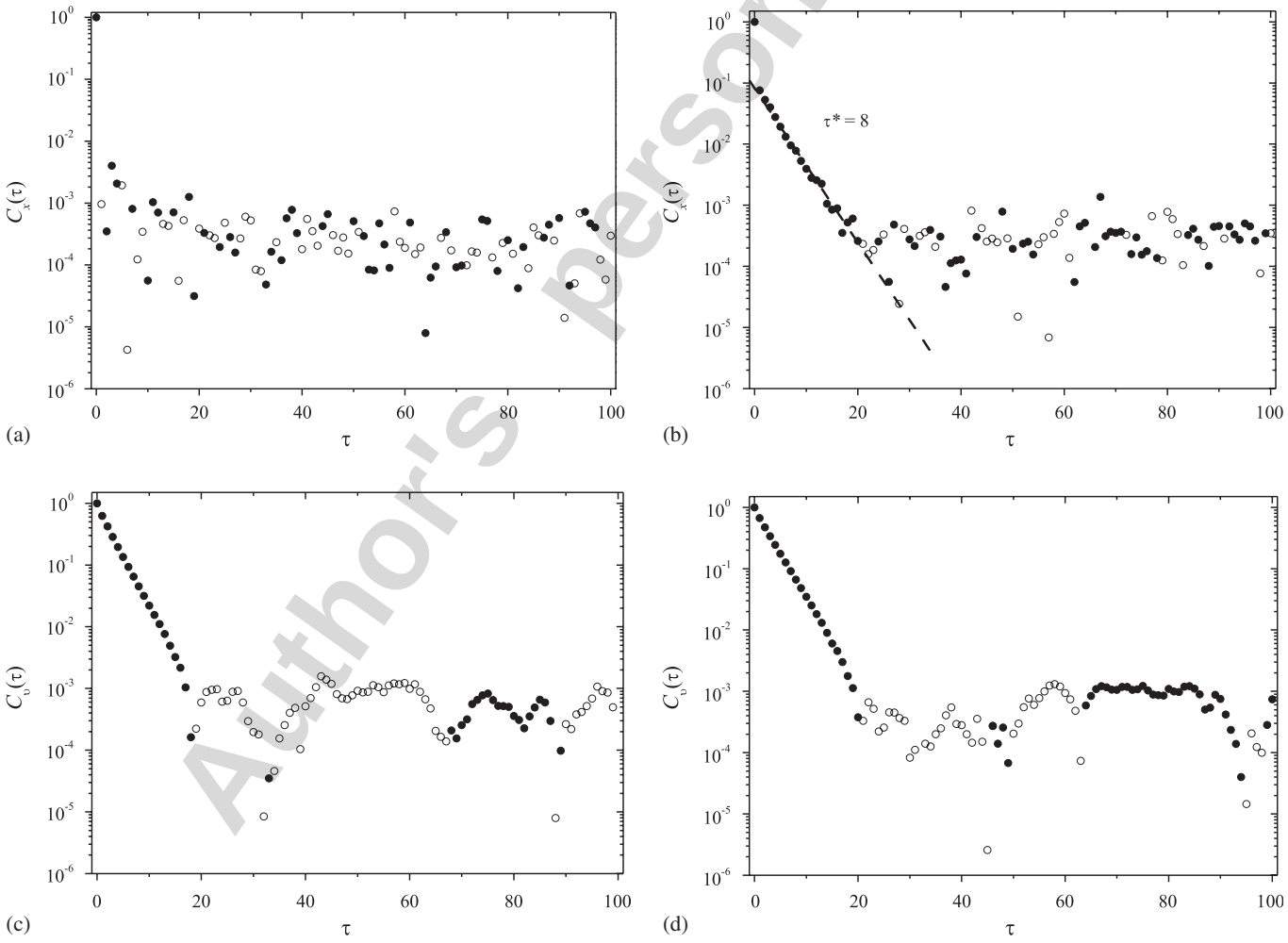

Fig. 5. Absolute values of the autocorrelation functions of returns $C_x(\tau)$ and volatilities $C_v(\tau)$, for the cases $B = 0$ [(a) and (c)] and $B = 0.25$ [(b) and (d)]. Full (empty) circles represent positive (negative) values of the correlations. In all cases, the values $A = 1.5$ and $h = 0.01$ were used.

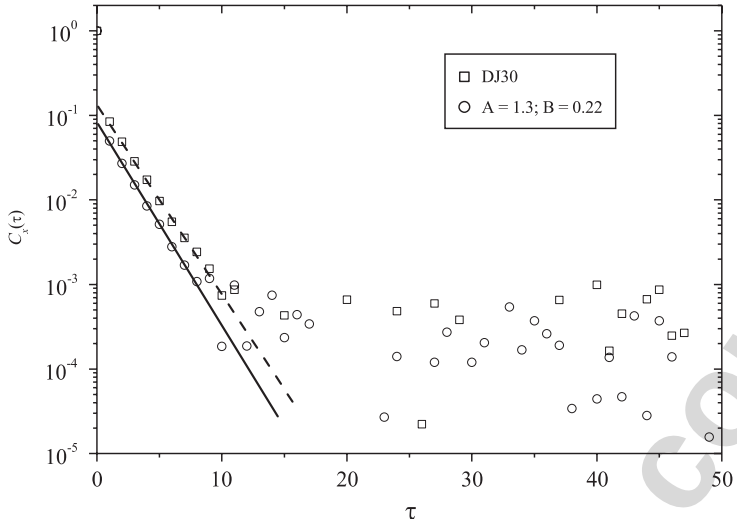

Fig. 6. The absolute value of the autocorrelation function of returns $C_x(\tau)$ from DJ30 data (squares) is compared with the one obtained through the present model using the parameters $A = 1.3$, $B = 0.22$, and $h = 0.01$ (circles).

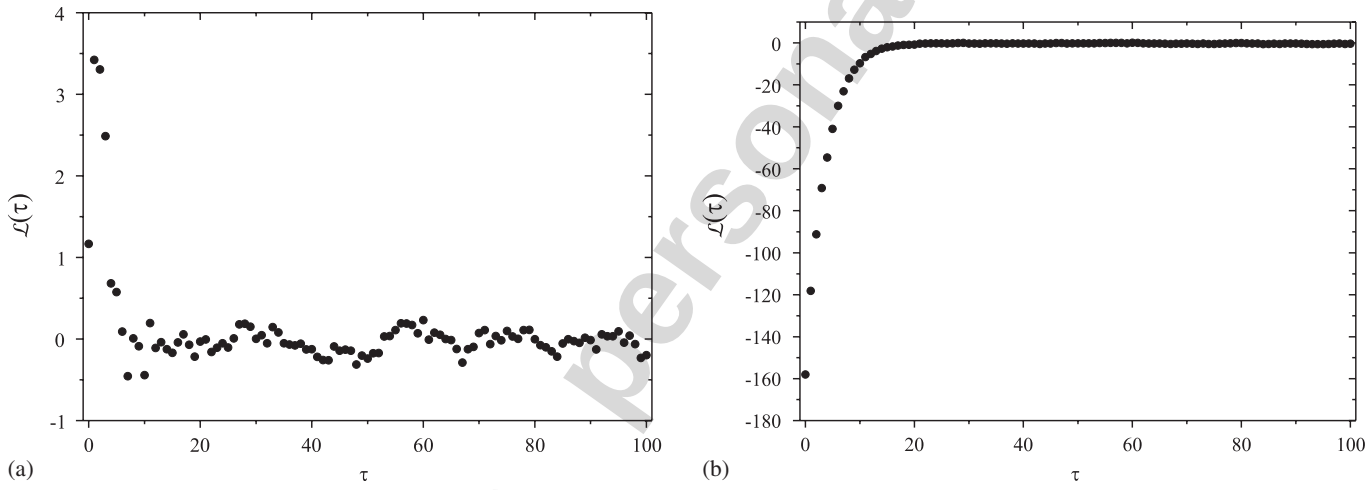

Fig. 7. The leverage correlation function $\mathscr{L}(\tau)$, for the cases (a) $B = 0$; (b) $B = 0.25$. In both cases, the values $A = 1.5$ and $h = 0.01$ were used.

Fig. 6), $\tau^* = 4.50 \pm 0.18$ min. Now, if one computes $C_x(\tau)$ from a time series generated by our model, with the parameters previously calculated from DJ30 data, i.e., $A = 1.3$, $B = 0.22$, and $h = 0.01$, one finds (from full straight line in Fig. 6), $\tau^* = 4.19 \pm 0.15$ [in arbitrary time units, as defined by Eq. (8)]. Therefore, if one sets 1 min as the unit of time in Eq. (8), our estimate for the correlation function $C_x(\tau)$ agrees, within the error bars, with the real one.

The leverage correlation function $\mathscr{L}(\tau)$, which measures the correlations between past returns and future volatilities, is presented in Fig. 7 for $B = 0$ [Fig. 7(a)] and $B = 0.25$ [Fig. 7(b)]. The leverage effect, which corresponds to a negative correlation between past returns and future volatilities, may be reproduced by considering $B > 0$. In Fig. 7(a) one notices a simple noisy pattern, whereas in Fig. 7(b) one observes a behavior similar to the empirical correlation for stock indices (see, e.g., Ref. [10, Fig. 2]). Such an empirical behavior is well fitted by the function $\mathscr{L}(\tau) = -A\exp(-\tau/\tau')$, which defines a characteristic time, τ'.

Finally, we have also analyzed some of our results, namely, the correlation functions $C_x(\tau)$ and $\mathscr{L}(\tau)$, for different values of the parameter B. We have verified that the associated characteristic times, τ^* and τ', may depend, in general, on the particular choices for the parameters (A, h, B). In order to illustrate the dependence to these characteristic times on B, in Fig. 8, we plot $(\tau^*)^{-1}$ and $(\tau')^{-1}$ for several values of B in the range [0.1,1.0], considering $A = 1.3$ and $h = 0.01$. The error bars, which represent uncertainties in the fits for the

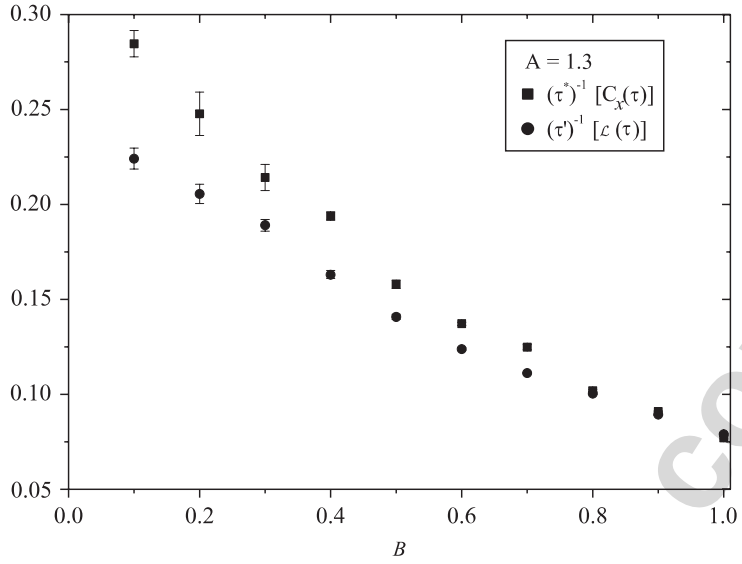

Fig. 8. The inverse of the characteristic times τ^* (squares) and τ' (circles), associated with the correlation functions $C_x(\tau)$ and $\mathscr{L}(\tau)$, respectively, are plotted for several values of B in the range [0.1,1.0]. The remaining parameters of Eq. (6) were fixed at $A = 1.3$ and $h = 0.01$. For $B \geqslant 0.4$, the error bars become smaller than the symbol sizes.

determination of these quantities, become smaller than the symbol sizes for $B \geqslant 0.4$. One notices that both $(\tau^*)^{-1}$ and $(\tau')^{-1}$ approach zero, for increasing values of B (typically, for $B \sim 1$), indicating the ceasing of validity for the exponential behavior of such correlation functions. It is important to stress that $B \sim 1$ is well above the appropriated range of values of B, mentioned in the beginning of the present section, to be used for a satisfactory description of empirical data.

4. Conclusions

We have introduced a multi-interacting agent model, for the description of financial markets. The model takes into account random interactions among the agents, including a *significant term* that measures the volatility of the market. This new term contributes to adjust the agents in such a way to avoid large return variations, taking into account a very important ingredient of financial markets, known as aversion to risk. The model resembles, within the magnetic language, an Ising random magnetic model with infinite-range interactions. We have shown that, the introduction of the volatility-like field term, provides a substantial improvement, leading to important qualitative changes with respect to previous works in the literature. The present model is able to reproduce the empirical behavior of several aspects of a real financial market: (i) non-Gaussian probability distribution of returns, characterized by a nonzero skewness; (ii) exponential decay of the two-time autocorrelation function of returns; (iii) negative correlations between past returns and future volatilities (leverage effect). We have verified that the results obtained from data of the present model are in good agreement with those obtained from one-minute return time series of the 30 most important individual stocks of Dow Jones index. It appears to be surprisingly that such a simple microscopic model is able to reproduce, so accurately, many features together of a real financial market. Although some methods that enable the emergence of the long-time power-law behavior observed empirically in the two-time autocorrelation function of volatilities have already been introduced [45–48], its appearance through microscopic multi-interacting agent models of financial markets remains as a challenge for future investigations.

Acknowledgments

It is a pleasure to thank C. Tsallis for fruitful conversations. F.D.N. is grateful to CBPF (Centro Brasileiro de Pesquisas Físicas) for the warm hospitality during a visiting period in which this work was developed. The

partial financial supports from CNPq and FAPERJ/PRONEX (Brazilian agencies) are acknowledged. S.M.D.Q. thanks the financial support from FCT/MCES (Portuguese agency).

Appendix A. Analysis of the maps in Eqs. (8) and (9)

In this appendix we will discuss in detail the map obtained through the application of the mean-field approach for the model discussed above [cf. Eq. (8)],

$$x(t+1) = \tanh[A\xi(t)x(t) + h\zeta(t) - B|x(t)|]. \tag{A.1}$$

For small arguments, $|A\xi(t)x(t) - B|x(t)| + h\zeta(t)| \ll 1$, this map may be written in its linearized form [cf. Eq. (9)],

$$x(t+1) \approx A\xi(t)x(t) + h\zeta(t) - B|x(t)|. \tag{A.2}$$

Depending on the choices of the parameters (A, h, B), the maps in Eqs. (A.1) and (A.2) may be dominated by well-defined fixed points, or may present more complex behavior, like chaotic regimes. The onset of chaos, signalled by the maximum Lyapunov exponent, $\lambda_{\max}$, becoming positive, should take place at a threshold surface $A^*(h, B)$. For $B = 0$, these maps fall in a general class of maps that have been investigated extensively [29–31]. In the case $h = 0$, for a uniformly distributed noise $\xi(t)$ in the interval $(-1, 1)$, there is a fixed point at $x = 0$ for $A < A^*(0, 0)$ $[A^*(0, 0) = e = 2.718\ldots]$, whereas for $A \geqslant A^*(0, 0)$ this fixed point loses stability and one enters into the chaotic region. We have computed $\lambda_{\max}$ through the algorithm described in Ref. [49], for the maps above, and the results in the simplest case $h = B = 0$ are exhibited in Fig. 9. In this case, we have verified that both maps present essentially the same $\lambda_{\max}$ up to $A \approx 3$, which implies that the threshold value, $A^*(0, 0) = e = 2.718\ldots$, applies to both maps. However, beyond $A \approx 3$, the two maps present different estimates for $\lambda_{\max}$: whereas for the map of Eq. (A.1) the chaotic regime disappears at $A \approx 3.12$, with the fixed points $x = \pm 1$ becoming new attractors for larger values of A, the chaotic regime persists for wider ranges of A in the map of Eq. (A.2). Therefore, this later map presents a much richer behavior than the former and, for this reason, has been more investigated in the literature.

For $h = B = 0$, the map of Eq. (A.2), which was introduced in the context of intermittency [29–31], may present very interesting behavior, due to the multiplicative noise $\xi(t)$. In this case, the trajectories depart from a laminar phase ($x = 0$), when $A\xi > e$, and are reinjected towards $x = 0$, when $A\xi < e$, yielding the typical *on–off intermittency* behavior. The on–off regime is composed by rare sequences of large (on average) values of x separated by laminar phases of random length which, at the onset of intermittency, are characterized by a power-law distribution with an exponent $-\frac{3}{2}$ [29,31]. The introduction of the additive noise term, $h\zeta(t)$ (h small,

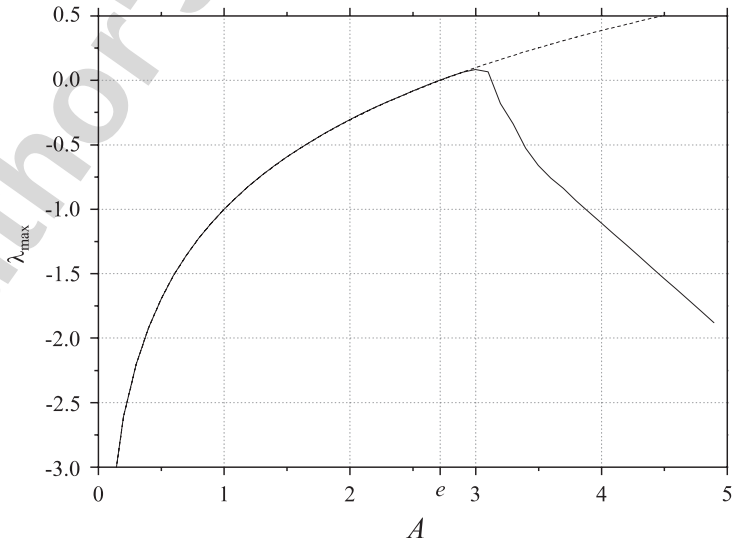

Fig. 9. The maximum Lyapunov exponent associated with the maps defined in Eqs. (A.1) (full line) and (A.1) (dashed line) is exhibited versus A, for the case $h = B = 0$.

typically, $h \approx 0.01$), leads to smaller values for the threshold of chaos, i.e., $A^*(h,0) < A^*(0,0)$; indeed, one finds $A^*(h,0) = 1$ for *any* additive noise [29–31]. In this case, for $A > 1$, the system is said to be in an *attractor bubbling* regime, where the additive noise is responsible for the bursts; the role of the multiplicative noise consists in the amplification of the bursts generated by the additive noise.

Let us now turn to the case $B > 0$. In Fig. 10 we exhibit $\lambda_{\max}$, computed through the algorithm of Ref. [49], for the maps above, in the case $h = 0$, and the estimated DJ30 average value of B, i.e., $B = 0.22$. The fact that the two estimates for $\lambda_{\max}$ are very close reflects the validity of the linear approximation. Surely, one of the effects of $B > 0$ is to restrict the validity of the linear approximation to smaller ranges of A; this is verified for $B = 0.22$, where the two maps present approximately the same $\lambda_{\max}$ up to $A \approx 2$, to be compared with $A \approx 3$, when $B = 0$. Through similar estimates of $\lambda_{\max}$, we have checked that for the range of B of interest in this paper ($0 \leqslant B \leqslant 0.35$), the two values of A used herein ($A = 1.5$ and 1.3) fall inside regions of validity of the linear approximation. From Fig. 10 one gets always $\lambda_{\max} < 0$ for the map of Eq. (A.1), leading to a complete suppression of the chaotic regime. However, for the map of Eq. (A.2), such a regime takes place for any $A > A^*(0, 0.22)$, where $A^*(0, 0.22) \approx A^*(0,0) = e = 2.718\ldots$ [in fact, we have computed $A^*(0, 0.22)$ up to two decimal places, $A^*(0, 0.22) \approx 2.72$]. Similarly to what happens in the case $B = 0$, the introduction of an additive noise term, $h\zeta(t)$, leads to smaller values for the threshold of chaos. For $h = 0.01$ and $B = 0.22$, we have estimated, up to two decimal places, the same threshold of chaos as in the case $B = 0$, $A^*(0.01, 0.22) \approx 1.00$. Since the parameter B does not bring any external noise to the maps above, the on-off intermittency [produced by the multiplicative noise term $A\xi(t)$] and attractor bubbling [produced by the additive noise term $h\zeta(t)$] regimes are still present for $B > 0$. Therefore, apart from the expected shrinking of the range of the A parameter, along which the linear approximation is expected to remain valid, the introduction of the new term $B|x(t)|$ does not change significantly the stability properties of the maps of Eqs. (A.1) and (A.2), at least for the magnitudes of B of interest in the present paper.

Let us now derive a simple equation relating the exponents of the tails of the probability distribution associated with the map of Eq. (A.2), in the case $h = 0$, with the parameters A and B. Since this map presents two branches, each one of them being similar to the multiplicative-noise map studied in Ref. [32], we assume that the probability density function presents the following asymptotic behavior,

$$P(x) \sim \begin{cases} |x|^{-\alpha-1} & \text{if } x < 0, \\ |x|^{-\beta-1} & \text{if } x \geqslant 0, \end{cases} \tag{A.3}$$

where, in principle, $\alpha \neq \beta$, since the dynamics for the positive and negative parts may be different. Carrying out the change of variables $y = \ln|x|$, and imposing the conservation of probabilities [$P(x)\,\mathrm{d}x = p(y)\,\mathrm{d}y$] for each

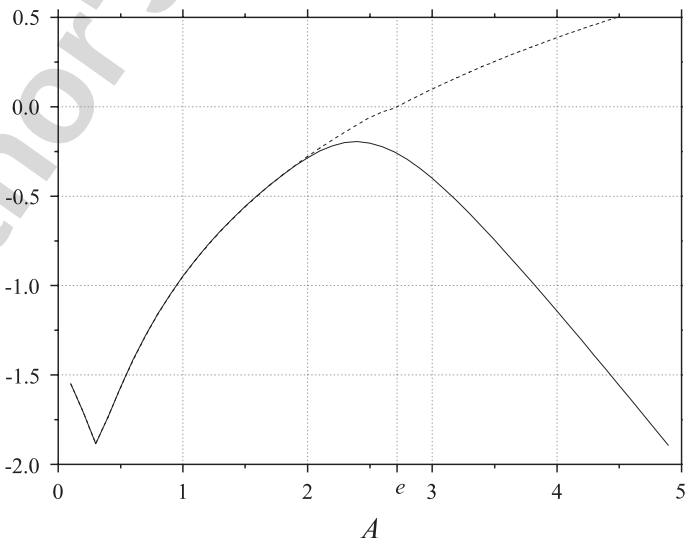

Fig. 10. The maximum Lyapunov exponent associated with the maps defined in Eqs. (A.1) (full line) and (A.1) (dashed line) is exhibited versus A, for the case $h = 0$ and $B = 0.22$.

of the parts in the equation above, one gets

$$p^{-}(y)\sim e^{-\alpha y}, \quad p^{+}(y)\sim e^{-\beta y}, \tag{A.4}$$

where the $-(+)$ notation applies to the y variable associated with $x<0$ ($x>0$). Considering the fact that the new variable y may be obtained from both positive and negative values of x, the full probability density function for y, in its asymptotic regime, should be proportional to the sum of $p^{-}(y)$ and $p^{+}(y)$, i.e.,

$$P(y) \propto e^{-\alpha y} + e^{-\beta y}. \tag{A.5}$$

Let us now consider the map of Eq. (A.2) in the case $h = 0$; taking the absolute value on both sides and splitting the contributions for negative and positive values of $x(t)$,

$$\begin{cases} |x(t+1)| \approx |(A\xi(t) + B)x(t)| & \text{if } x<0, \\ |x(t+1)| \approx |(A\xi(t) - B)x(t)| & \text{if } x\geqslant 0, \end{cases} \tag{A.6}$$

and then, applying the logarithm on both sides,

$$\begin{cases} y(t+1) \approx \ln|A\xi(t) + B| + y(t) & \text{if } x<0, \\ y(t+1) \approx \ln|A\xi(t) - B| + y(t) & \text{if } x\geqslant 0, \end{cases} \tag{A.7}$$

where we have used $y(t) = \ln|x(t)|$.

In the analysis that follows we shall restrict ourselves to parameters $A>B>0$, which corresponds to the situation of interest in the present paper. Defining $z = |A\xi + B|$, $z' = |A\xi - B|$, and reminding that ξ is a uniform random variable in the interval $(-1, 1)$, one immediately verifies that the probability distributions associated with these variables are given by

$$P(z) \equiv P(z') = \begin{cases} 1/A & \text{if } 0<z, z'<|A - B|, \\ 1/(2A) & \text{if } |A - B|<z, z'<|A + B|. \end{cases} \tag{A.8}$$

Now, for a variable $w = \eta, \eta'$, where $\eta = \ln z$ and $\eta' = \ln z'$, one obtains,

$$p(w) = \begin{cases} [1/A]\exp(w) & \text{if } -\infty<w<\ln|A - B|, \\ [1/(2A)]\exp(w) & \text{if } \ln|A - B|<w<\ln|A + B|. \end{cases} \tag{A.9}$$

From (A.7) one gets that the probability $P[y(t+1)]$, for obtaining the variable y at time $t+1$, is given by summing the contributions from $x>0$ and $x<0$; the contribution for $x<0$ ($x>0$) results from an integration over all possible values of $y(t)$ and $\eta(t)$ ($\eta'(t)$). In other words,

$$\begin{aligned} P[y(t+1)] \propto & \int p^{-}[y(t)]p[\eta(t)]\delta\{y(t+1) - y(t) - \eta(t)\}\,dy(t)\,d\eta(t) \\ & + \int p^{+}[y(t)]p[\eta'(t)]\delta\{y(t+1) - y(t) - \eta'(t)\}\,dy(t)\,d\eta'(t), \end{aligned} \tag{A.10}$$

which, after using Eq. (A.4), results in

$$\begin{aligned} P[y(t+1)] \propto & \exp[-\alpha y(t+1)] \int p[\eta(t)]\exp[\alpha\eta(t)]\,d\eta(t) \\ & + \exp[-\beta y(t+1)] \int p[\eta'(t)]\exp[\beta\eta'(t)]\,d\eta'(t). \end{aligned} \tag{A.11}$$

Comparing Eqs. (A.5) and (A.11), one gets

$$\int p[\eta(t)]\exp[\alpha\eta(t)]\,d\eta(t) = \int p[\eta'(t)]\exp[\beta\eta'(t)]\,d\eta'(t) = 1. \tag{A.12}$$

Since $p(\eta) = p(\eta')$, the two integrals above are equivalent. Therefore, $\alpha = \beta$, i.e., the asymptotic behavior of the probability distribution $P(x)$ [cf. Eq. (A.3)] follow a power-law with the same exponent α for both positive and

negative values of x. By solving Eq. (A.12), one gets the following relation:

$$\frac{(A-B)^{1+\alpha}+(A+B)^{1+\alpha}}{2A(1+\alpha)}=1, \tag{A.13}$$

which is used in the main text.

References

[1] R.N. Mantegna, H.E. Stanley, An Introduction to Econophysics: Correlations and Complexity in Finance, Cambridge University Press, Cambridge, 1999.
[2] J.P. Bouchaud, M. Potters, Theory of Financial Risks: From Statistical Physics to Risk Management, Cambridge University Press, Cambridge, 2000.
[3] J. Voit, The Statistical Mechanics of Financial Markets, second ed., Springer, Heidelberg, 2003.
[4] B.B. Mandelbrot, Fractals and Scaling in Finance, Springer, New York, 1997.
[5] H.E. Santley, L.A.N. Amaral, X. Gabaix, P. Gopikrishnan, V. Plerou, Physica A 299 (2001) 1.
[6] P. Gopikrishnan, V. Plerou, L.A.N. Amaral, M. Meyer, H.E. Stanley, Phys. Rev. E 60 (1999) 5305.
[7] R.N. Mantegna, H.E. Stanley, Phys. Rev. Lett. 73 (1994) 2946.
[8] R.N. Mantegna, H.E. Stanley, Nature 376 (1995) 46.
[9] L.C. Miranda, R. Riera, Physica A 297 (2001) 509.
[10] J.-P. Bouchaud, A. Matacz, M. Potters, Phys. Rev. Lett. 87 (2001) 228701.
[11] S.L. Heston, Rev. Financial Stud. 6 (1993) 327.
[12] J.-P. Bouchaud, R. Cont, Eur. Phys. J. B 6 (1998) 543.
[13] S.M.D. Queirós, C. Anteneodo, C. Tsallis, in: D. Abbot, J.-P. Bouchaud, X. Gabaix, J.L. McCauley (Eds.), Noise and Fluctuations in Econophysics and Finance, SPIE, Bellingham, WA, 2005, p. 151.
[14] L. Borland, Phys. Rev. Lett. 89 (2002) 098701.
[15] L. Borland, J.-P. Bouchaud, Quant. Finance 4 (2004) 499.
[16] T. Lux, M. Marchesi, Nature 397 (1999) 498.
[17] K. Sznajd-Weron, J. Sznajd, Int. J. Mod. Phys. C 11 (2000) 1157.
[18] S. Bornhold, Int. J. Mod. Phys. C 12 (2001) 667.
[19] G. Iori, J. Econ. Behav. Organ. 49 (2002) 269.
[20] A. Krawiecki, J.A. Holyst, D. Helbing, Phys. Rev. Lett. 89 (2002) 158701.
[21] B. Rosenow, P. Gopikrishnan, V. Plerou, H.E. Stanley, Physica A 314 (2002) 762.
[22] L. Sabatelli, P. Richmond, Physica A 344 (2004) 62.
[23] A.P. Young (Ed.), Spin Glasses and Random Fields, World Scientific, Singapore, 1998.
[24] K.H. Fischer, J.A. Hertz, Spin Glasses, Cambridge University Press, Cambridge, 1991.
[25] K. Binder, A.P. Young, Rev. Mod. Phys. 58 (1986) 801.
[26] J.P. Bouchaud, Physica A 313 (2002) 238.
[27] D.J. Amit, Modeling Brain Function, Cambridge University Press, Cambridge, 1989.
[28] P. Peretto, An Introduction to the Modeling of Neural Networks, Cambridge University Press, Cambridge, 1992.
[29] N. Platt, E.A. Spiegel, C. Tresser, Phys. Rev. Lett. 70 (1993) 279.
[30] N. Platt, S.M. Hammel, J.F. Heagy, Phys. Rev. Lett. 72 (1994) 3498.
[31] J.F. Heagy, N. Platt, S.M. Hammel, Phys. Rev. E 49 (1994) 1140.
[32] Y. Kuramoto, H. Nakao, Phys. Rev. Lett. 78 (1997) 4039.
[33] H. Nakao, Phys. Rev. E 58 (1998) 1591.
[34] B.M. Hill, Ann. Stat. 3 (1975) 1163.
[35] D. Prato, C. Tsallis, Phys. Rev. E 60 (1999) 2398.
[36] C. Tsallis, Braz. J. Phys. 29 (1999) 1.
[37] C. Anteneodo, C. Tsallis, J. Math. Phys. 44 (2003) 5194.
[38] M. Potters, R. Cont, J.-P. Bouchaud, Europhysics Lett. 41 (1998) 239.
[39] B.B. Mandelbrot, J. Bus. 36 (1963) 394.
[40] G.M. Viswanathan, U.L. Fulco, M.L. Lyra, M. Serva, Physica A 329 (2003) 273.
[41] S.M.D. Queirós, Quant. Finance 5 (2005) 475.
[42] M. Pasquini, M. Serva, Econ. Lett. 65 (1999) 275.
[43] M. Pasquini, M. Serva, Eur. Phys. J. B 16 (2000) 195.
[44] M. Serva, U.L. Fulco, M.L. Lyra, F. Petroni, G.M. Viswanathan, Physica A 363 (2006) 393.
[45] S. Ghahghaie, W. Breymann, J. Peinke, P. Talkner, Y. Dodge, Nature 381 (1996) 767.
[46] J.-F. Muzi, J. Delour, E. Bacry, Eur. Phys. J. B 17 (2000) 537.
[47] A. Arneodo, J.-F. Muzi, D. Sornette, Eur. Phys. J. B 2 (1998) 277.
[48] J.P. Bouchaud, M. Potters, M. Meyer, Eur. Phys. J. B 13 (1999) 595.
[49] G. Benettin, L. Galgani, J.M. Strelcyn, Phys. Rev. A 14 (1976) 2338.